Indian J. Phys. **70A** (1), 81–89 (1996)

IJP A
an international journal

Deformed configuration mixing shell model in medium heavy nuclei

R Sahu
Physics Department, Berhampur University,
Berhampur-760 007, India

Abstract : We discuss here the application of the deformed configuration mixing shell model based on HF states to study spectroscopic properties of nuclei, inelastic electron scattering, spectroscopic factors etc

Keyword : Deformed configuration mixing shell model, medium heavy nuclei, spectroscopic properties

PACS No. : 21 60 Cs

1. Introduction

Professor S P Pandya [1] has already discussed about the developments of the deformed configuration mixing shell model. I will here mainly confine my attention to the application of this model. We have applied this model to study the nuclear energy levels and electromagnetic properties of the nuclei in the $A = 80$ region. We have also applied this model to calculate the form factors in the inelastic electron scattering from *fp* shell nuclei. We are planning to calculate the spectroscopic factors in direct reactions. Each of the applications is discussed below.

2. Nuclear spectroscopy in the $A = 80$ region

The nuclei in the mass region $A = 60$–80 show very complex and interesting structures with properties such as large ground-state deformation, coexistence of shapes, band crossing *etc*. Hence they have attracted considerable attention over the last few years. Most of the $N = Z$ nuclei in this region lie far from the valley of stability. Hence they are increasingly difficult to access as the mass number A increases. However with the development of new accelerators and sensitive detector systems, it has recently become possible to experimentally study such nuclei. These $N = Z$ nuclei are particularly of special interest since shell effects occur simultaneously for both protons and neutrons. Recently Lister and

his collaborators [2] have experimentally studied the self-conjugate nucleus ^{64}Ge. They have observed a ground band extending upto $J = 8^+$, a quasigamma band and a $K = 3^-$ band. From their theoretical analysis, they found this nucleus to have large triaxiality with $\beta \simeq 0.22$. The details of the calculation have been discussed by Professor Pandya. I give here only a few important steps. In our calculation, we take ^{56}Ni as the inert core. The active configuration space is made of the single particle orbits $^1p_{3/2}$, $^0f_{5/2}$, $^1p_{1/2}$ and $^0g_{9/2}$. The spherical single particle energies for these levels are taken as 0.0, 0.78, 1.08 and 3.5 MeV. As in our earlier calculations, we use a modified Kuo interaction. We first solve the HF equations self consistently and generate the lowest prolate and oblate intrinsic states. Various excited intrinsic states are generated by making $1p1h$ and $2p2h$ excitations over the lowest prolate and oblate states. Good angular momentum states are projected from each of these intrinsic states. These projected states are, in general, not orthogonal to each other. They are orthonormalized following the standard prescription. These levels are classified into different bands on the basis of the $B(E2)$ values among them. The comparison between experiment and theory are given in Figure 1(a, b) for positive and negative parity

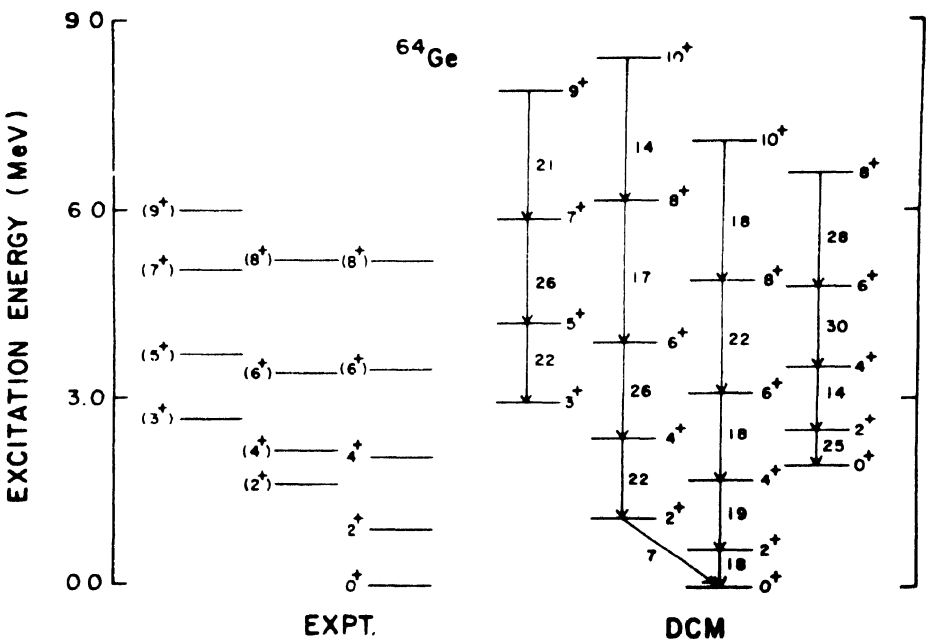

Figure 1(a). Comparison between experimental and calculated collective bands. The quantities near the arrows represent the $B(E2)$ values in W.U positive parity.

bands. The calculated lowest $K = 0^+$ band agrees quite well with experiment. Except for the $2^+ \rightarrow 0^+$ separation, the relative spacing of all the levels are well reproduced. Since we consider only axially symmetric HF states, we can not directly comment regarding the triaxiality of this nucleus However as we go to higher spins in the ground band, there is considerable mixing from the $K = 2^+$ and $K = 4^+$ bands. This, in a way suggests that this nucleus is triaxial in the ground band. The $K = 2^+$ band is quite nicely reproduced.

Except for the lowest 3^- level, all the other negative parity bands are well described in our model.

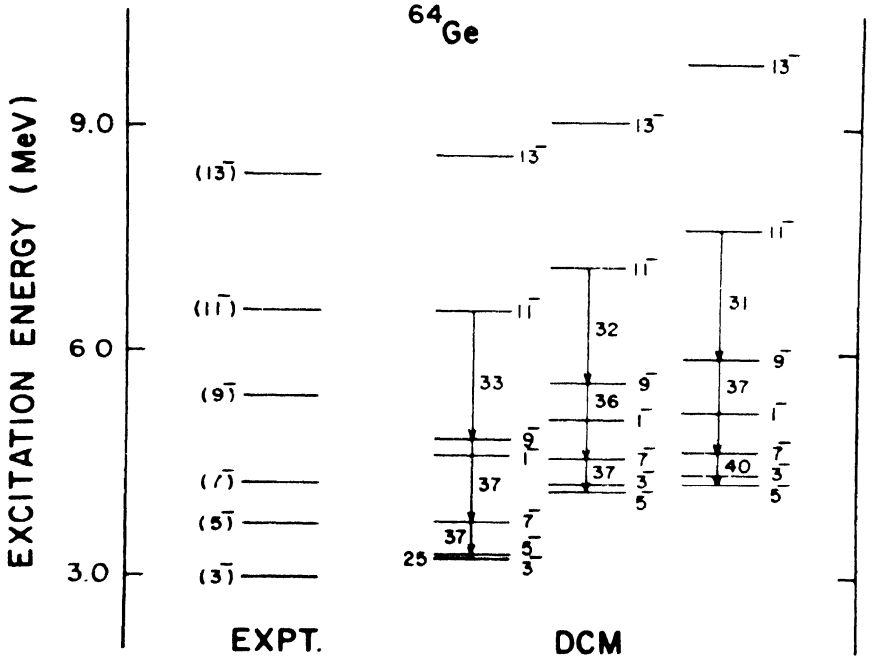

Figure 1(b). Comparison between experimental and calculated collective bands. The quantities near the arrows represent the $B(E2)$ values in W.U. negative parity

3. Inelastic electron scattering

Electron scattering has been a powerful tool for studying nuclear structure. The basic interaction of the electron with the constituents of the nucleus is well known and relatively weak. Hence one can make measurements on the target nucleus without greatly disturbing its structure. The cross sections associated with the population of a particular nuclear state in electron scattering are basically the Fourier transform of the transition charge and current densities. The spatial distribution of these densities provide a significant insight into the structure of the target nucleus.

The general theory of the scattering of electrons from nuclei has been discussed in detail by many authors [3]. Most of the theoretical treatments are based on the Born approximation. Since the incoming and outgoing electron waves are distorted by the coulomb field of the nucleus, one should, in principle, perform the calculation using the distorted wave Born approximation. However, electron scattering is often treated within the framework of the plane wave Born approximation since it gives better physical insight. The cross section for the scattering of an electron from a nucleus of charge Z is given as

$$\frac{d\sigma}{d\Omega} = \sigma_M \left[\sum_{\lambda=0}^{\infty} \left| F_\lambda^{LL}(q) \right|^2 + \left(\frac{1}{2} + \tan^2 \frac{\theta}{2} \right) \sum_{\lambda=1}^{\infty} \left\{ \left| F_\lambda^{TL}(q) \right|^2 + \left| F_\lambda^{TM}(q) \right|^2 \right\} \right] \tag{1}$$

Here σ_M is the Mott cross section which correspond to the relativistic elastic electron scattering cross section from a point charge and contains most of the kinematics. The nuclear structure informations are contained in the form factors. In the above F^{LE}, F^{TE} and F^{TM} are, respectively, the longitudinal electric, transverse electric, and transverse magnetic form factors. The transverse form factors are quite negligible for the lowlying collective states with which we shall mainly be concerned. For a given momentum transfer q, the longitudinal electric form factor is given by

$$F_\lambda(q) = \frac{1}{Z^2} \left\langle \psi^k_{I_f M_f} \right| \sum_{k=1}^{A} \frac{1}{2} \left[(1+\tau^k) e_p + (1-\tau^k) e_n \right] e^{iq \cdot r_k} \left| \psi^k_{I_i M_i} \right\rangle \tag{2}$$

where $\psi^k_{I_i M_i}$ and $\psi^k_{I_f M_f}$ are the initial and final nuclear functions, $\tau^k = 1$ for protons and $\tau^k = -1$ for neutrons. Using the Rayleigh expansion and summing over the final states and averaging over the initial states, one obtains the expression for the square of the form factor of multipolarity λ as

$$\left|F_\lambda(q)\right|^2 = \frac{4\pi}{Z^2} \frac{1}{2I_i+1} \sum_{\lambda} \left\langle \psi^k_{I_f} \right| \left| \frac{1}{2} \sum_{k} \left[(1+\tau^k) e_p + (1-\tau^k) e_n \right] j_\lambda(qr) Y_\lambda(\Omega) \right| \left| \psi^k_{I_i} \right\rangle \tag{3}$$

The above expression reduces to that for $B(E\lambda)$ if $j_\lambda(qr)$ is replaced by r^λ and the constant term $4\pi/Z^2$ is set to unity. The evaluation of this expression within the HF approximation is discussed in ref. [4]. We make the standard corrections due to the finite size of the proton and the center of mass correction and the correction due to the use of PWBA. The calculations are made within a model space $^0f_{7/2}$, $^1p_{3/2}$, $^0f_{5/2}$, $^1p_{1/2}$ with ^{40}Ca as the core. A modified Kuo-Brown effective interaction lavelled MWH2 is employed.

3.1. *Form factor for the $0^+ \rightarrow 2^+$ transition*

In the last few years, a large amount of data has been collected for the $C2$ form factor. For almost all the nuclei in the *fp* shell, one observes three peaks in the form factor for the excitation of the first 2^+ state. The first peak appears at $q = 0.7\,fm^{-1}$, the second peak at 1.7 fm^{-1} and the third peak appears at a momentum transfer of 2.6 fm^{-1}. Most of the theoretical calculations fit the effective charges for each nucleus so as to correctly reproduce the peaks.

The effective charges are introduced to take into account the effects of core polarization and limited basis space. Within a given mass region, effective charges should almost be constant. If one changes the effective charges for neighbouring nuclei, then these effective charges would be no more than the adjustable parameters and much of the beauty of the microscopic calculation will be lost. Dhar and Bhatt [4] have shown that the B ($E2$) values and quadrupole moments of the isotopes of Ti, V, Cr and Fe can be reproduced by taking effective charges $e_p = 1.33\,e$ and $e_n = 0.64\,e$. We take these effective charges to calculate the form factors for the transition $0^+ \rightarrow 2^+$. The results are shown in Figures 2 – 4. The

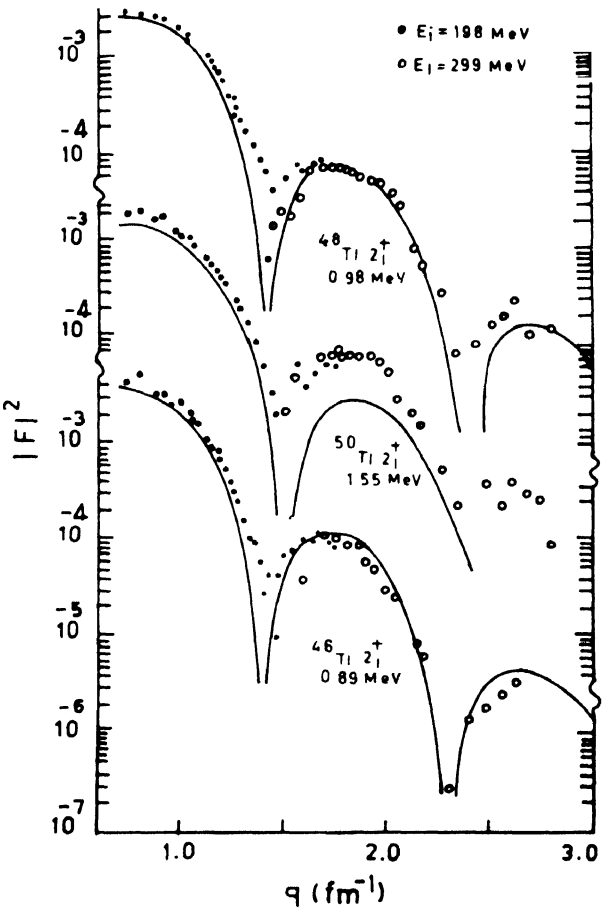

Figure 2. Comparison between calculated and experimental form factor for the $0^+ \rightarrow 2^+$ transition in ^{46,48,50}Ti. The experimental data at E_i = 198 MeV are represented by points and those at E_i = 299 MeV by open circles.

agreement in most cases is quite satisfactory. Most of the disagreements occur at large momentum transfer. This may be due to the PWBA formalism we have used. DWBA may help. Again we have taken only the lowest HF state in the above calculation. Taking a few excited intrinsic states and performing a band mixing calculation may improve the results.

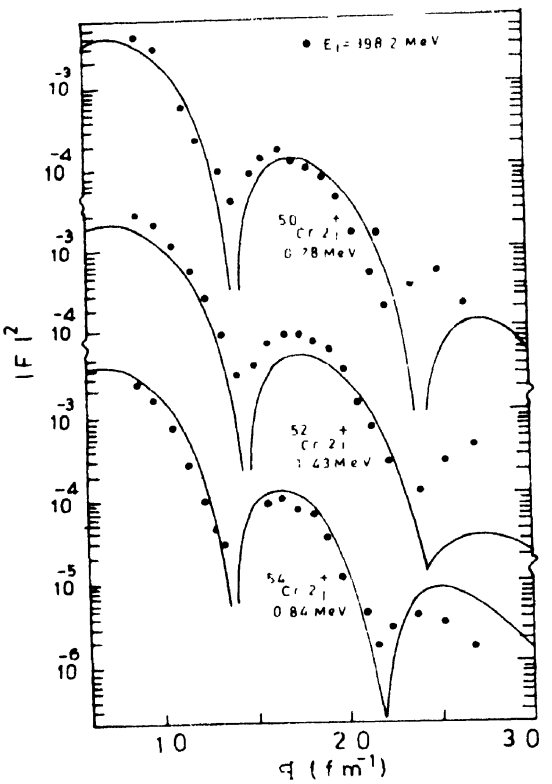

Figure 3. Comparison between calculated and experimental form factors for the $0^+ \rightarrow 2^+$ transition in ^{50,52,54}Cr. The experimental data at E_l = 398 2 MeV are represented by points

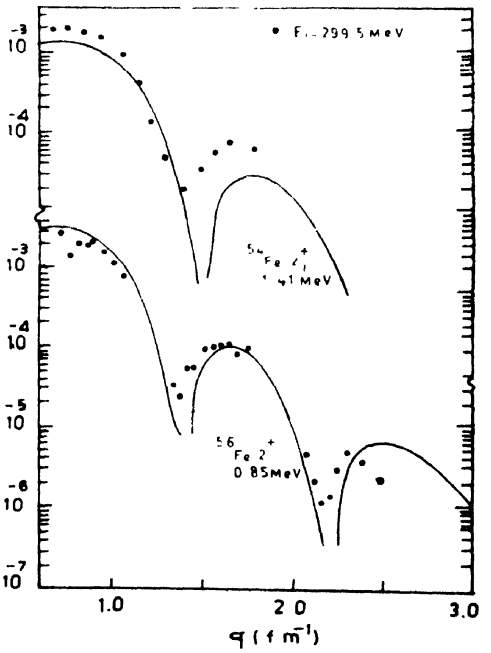

Figure 4. As in Figure 2 but for ^{54,56}Fe and E_l = 299 5 MeV.

3.2. Form factor for the transition $0^+ \rightarrow 6^+$

The effective charges for this transition are obtained using a least square fit between calculated and experimental B ($E6$) values. The effective charges, so obtained, are $e_p = 1.04$ e and $e_n = 0.29$ e. These effective charges reproduce the experimental B ($E6$) values quite

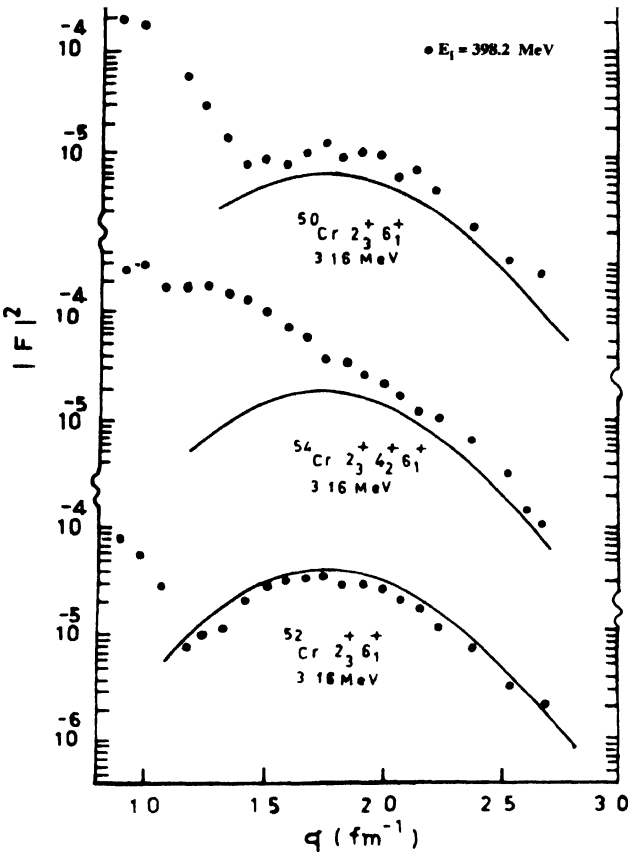

Figure 5. Comparison between calculated and experimental form factors for the $0^+ \rightarrow 6^+$ transition in ^{50,52,54}Cr (E_i = 398.2 MeV for the experimental points).

well. The $C6$ form factors calculated with the above effective charges are compared with experiment in Figure 5 for ^{50,52,54}Cr. We are able to reproduce only the second peak. Other calculations also fail to explain the first peak.For each of the above nuclei, there exists a 2^+ state close to the 6^+. The first peak may be due to the 2^+.

3.3. Form factor for $0^+ \rightarrow 4^+$ transition

The effective charges for this transition are calculated by a least square fit with the experimental B ($E4$) values. The calculated form factors for this transition are calculated

with experiment in Figure 6. Though we are able to produce the peaks, we do not get quantitative agreement.

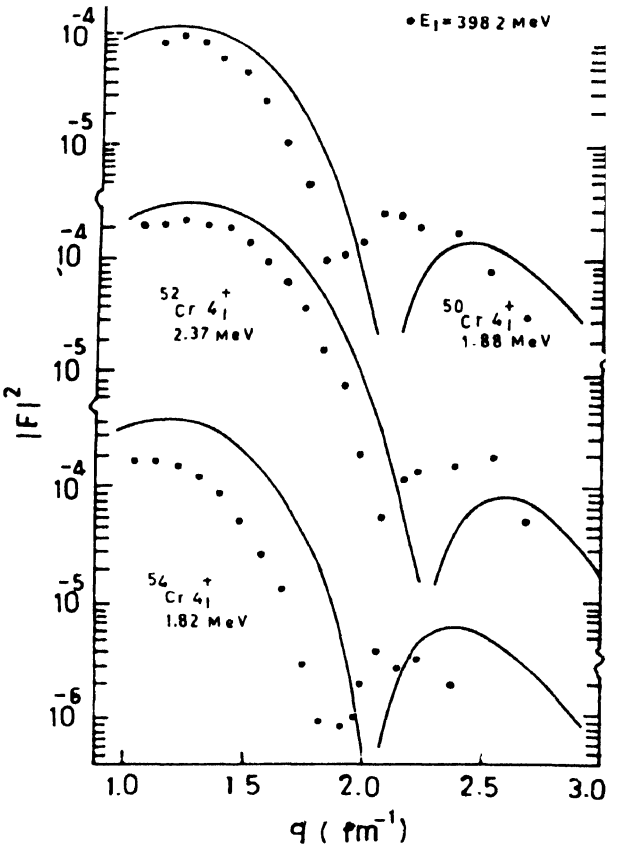

Figure 6. Comparison between calculated and experimental form factors for the $0^+ \rightarrow 4^+$ transition in ^{50,52,54}Cr (E_i = 398.2 MeV for experimental points)

4. Spectroscopic factor

The spectroscopic factor S for stripping reactions can be expressed as [5]

$$S(\rho) = n[I(\rho)]^2 \tag{4}$$

Here the symbol ρ specifies all quantum numbers of the transferred nucleon and n is the number of active particles in the final state. The overlap integral $I(\rho)$ is defined as

$$I(\rho) = \left\langle \left[\psi_{J_i}(1, \ldots, n-1) \times \rho(n) \right]^{J_f} \middle| \psi_{J_f}(1, \ldots, n) \right. \tag{5}$$

where the symbol x denotes vector coupling. Thus the value of $I(\rho)$ depends on the overlap between the final state $\psi_{J_f}(1, \ldots, n)$ (which is completely antisymmetric in the n active particles) and the state formed by coupling the initial state ψ_J (1, ..., n–1) (which is

antisymmetric in $n-1$ particles) with the transferred particle to a coupled-channel state ψ_{J_f}. Since we know the initial and final wave functions from our HF-projection calculation, the spectroscopic factor can easily be calculated. This calculation is in progress. For pickup reactions, we plan to follow a similar procedure.

5. Conclusion

We have described above the application of our deformed configuration mixing shell model to calculate different physical quantities. As has been discussed by Prof. Pandya, our approach is an approximation to shell model. Our model is capable of calculating all the quantities the shell model is capable of.

References

[1] S P Pandya *Invited talk given in the present workshop*

[2] P J Ennis *et al Nucl Phys* **A535** 392 (1991) ; S S L Ooi *et al Phys Rev* **C34** 1153 (1986) , C J Lister *et al Phys Rev* **C42** R1191 (1990)

[3] H Uberall *Electron Scattering from Complex Nuclei*, Academic press, New York (1971), T deForest (Jr) and J D Walecka *Adv Phys.* **15** 1 (1966)

[4] A K Dhar and K H Bhatt *Phys Rev* **C16** 792 (1977)

[5] P J Brussaard and P W M Glaudemans *Shell Model Applications in Nuclear Spectroscopy* (Amsterdam North Holland)